Passive Impedance Sensing Using a SAW Resonator-Coupled Biosensor for Zero-Power Wearable Applications

Xicai Yue, *Senior Member, IEEE*, Janice Kiely, Richard Luxton, Boyang Chen, Chris N. McLeod, *Member, IEEE*, and Emanuel Manos Drakakis, *Member, IEEE*

***Abstract*—A bio-sensing scheme, which acquires impedance information of a capacitive biosensor by using the reflected RF signal from a surface acoustic wave (SAW) resonator connected to the biosensor, is proposed. This technique requires no power to be supplied to the biosensor node and hence is highly applicable to wearable applications. Theoretical analysis has demonstrated that the sensitivity of the SAW resonator-coupled biosensor is higher than that of traditional impedance loaded SAW sensors and therefore it is more suitable for measuring the very small impedance changes in biosensors. The passive detection of the change in the impedance of a capacitive biosensor, as a result of biological binding events associated with the capture of a target analyte, has been demonstrated by preliminary experimentation. Dry tests of the SAW coupled capacitive biosensor using a cable connected network analyzer showed the aF level capacitance measurement resolution, which was only achieved in transistor level circuits previously, could be attained. When liquid samples with concentrations of C-Reactive Protein (CRP) in the range of 0.1 to 2 μg/ml were applied to the biosensor, a corresponding change in the resonant frequency of the SAW resonator-coupled biosensor (in the order of sub-hundred kHz) was observed. This has demonstrated the potential for applying this technique in applications where a zero-power requirement at the biosensor node could be a distinct advantage, when the cable link between the network analyzer and the biosensor node is replaced by the RF transmission.**

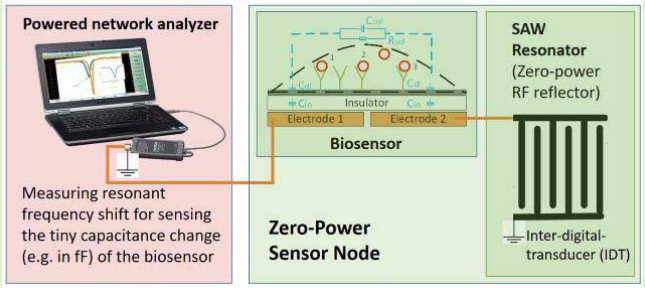

***Index Terms*— Biosensor, impedance, wearable device, passive sensing, zero-power communication, surface acoustic wave (SAW), resonator.**

I. Introduction

WEARABLE sensors and biosensors give information about the physiology and biochemical status of a person in real-time as the person interacts with their environment. This may be a person bedbound in a hospital or a sports person engaged in a physical activity. Wearable sensors measure physical and physiological parameters, such as temperature, heart rate, respiration, gait and biochemical changes, plus they can give environmental information, for example global position and speed through GPS interfaces. Many of these systems have been integrated in wearable devices, such as smart-watches. The measurement of biochemical parameters, such as glucose, lactate and hormones require a biosensor where an active biological layer on the sensor surface interacts with the target analyte. These wearable biosensors have been incorporated into contact lenses, gum-shields, spectacles, and fabricated into a patch worn on the skin for the measurement of compounds in sweat such as glucose, lactate and cortisol [1]. The advent of advanced materials that can be adapted for flexible electronics [2] has facilitated the development of a diverse range of biosensor technologies that are in contact with the skin, such as a "smart tattoo" [3] and sensors can be integrated with micro-

Manuscript received November 18, 2021; accepted December 5, 2021. Date of publication December 20, 2021; date of current version January 31, 2022. This work was supported by the Vice Chancellor's Early Career Researcher Development Awards, University of the West of England, Bristol. The associate editor coordinating the review of this article and approving it for publication was Prof. Aime Lay-Ekuakille. *(Corresponding author: Xicai Yue.)*

Xicai Yue is with the Department of Engineering Design and Mathematics, University of the West of England, Bristol, BS16 1QY, U.K. (e-mail: alex.yue@uwe.ac.uk).

Janice Kiely, Richard Luxton, and Boyang Chen are with the Institute of Bio-Sensing Technology, University of the West of England, Bristol BS16 1QY, U.K. (e-mail: janice.kiely@uwe.ac.uk; richard.luxton@uwe.ac.uk; boyang2.chen@live.uwe.ac.uk).

Chris N. McLeod is with the Department of Electrical and Electronics Engineering, Imperial College London, London SW7 2AZ, U.K. (e-mail: c.mcleod@imperial.ac.uk).

Emanuel Manos Drakakis is with the Department of Bioengineering, Imperial College London, London SW7 2AZ, U.K. (e-mail: e.drakakis@imeprial.ac.uk).

Digital Object Identifier 10.1109/JSEN.2021.3136705

needles that collect interstitial fluid just under the skin [4]. Many of these biosensors use electrochemical or impedimetric measurements depending on the analyte.

To measure impedance of a biosensor, an electrical source signal (e.g. a constant current) is injected and then the output voltage across the biosensor is recorded. Since the output voltage of a biosensor is composed of both real and imaginary components, a data demodulation process (commonly implemented by a digital signal processing (DSP) algorithm [5]) is necessary. The power consumption of a commercially available low-power solution of the system-on-chip (SoC) impedance converter of AD5933 [6] from Analog Devices is more than 30 mW when working at up to 100 kHz. More power is accordingly required when bioimpedance of a biosensor is measured at a higher frequency (e.g. up to 50 MHz [7]). Therefore power consumption of impedance measurement is an obstacle for biosensor's wearable applications where a battery is commonly employed as the power supply.

Energy harvesting and wireless power transfer provide potential ways of powering wearable biosensors. However, for most indoor applications the harvested power from a wearable indoor energy harvester (e.g. a commercially available credit card size photovoltaic energy harvester) is too weak for powering tens mW impedance measurement applications [8], while the most efficient wireless power transfer reported (40% efficiency and 4 times distance of coil diameter without requiring the clear line-of-sight [9]) using magnetic resonant coupling can only provide μW when size of the coil is reasonable to wear. Furthermore, the desired wireless communication link, such as minimum current requirement of 6 mA in Bluetooth Low Energy (BLE), requires extra power in mW, making the case of powering a wearable biosensor even worse. Fortunately, passive communication using radio frequency identification (RFID) provides a limited distance (tens of cm) zero-power wireless link [10], [11] under restricted coil alignment, but even after adopting RFID technology for communication the power consumption issue of impedance measurement of a biosensor for wearable applications remains.

Surface acoustic wave (SAW)-biosensors [12], which combine a SAW device with a microfluidic component, and which includes an extra biosensing layer on top of piezoelectric material of the SAW for binding specifically to the analyte, have been reported [13], [14]. These sensors can be interrogated remotely without a power supply required on the sensor side. These kind of SAW biosensors have been reported to have high sensitivity and fast response time, suitable for point of care applications. However, there are challenges associated with ensuring efficient electrochemical coupling between the SAW device and the biosensor surface, calling for a calibration-less method, which is convenient to use and most importantly suitable for mass production.

In contrast, the impedance loaded SAW sensor [15], [16] has been successfully commercialized, such as for remote, passive tyre pressure measurements. The recent report on using an implanted SAW resonator for remote measurement of blood pressure of post-surgery cardiac patients [17] inspire us to explore the feasibility of using a SAW linked biosensor to solve the high power consumption issue of impedance measurements through directly sensing (rather than measuring) the impedance of a biosensor with zero-power consumption. This zero-power solution also comes with the potential benefits of using commercially-available mass produced SAW components.

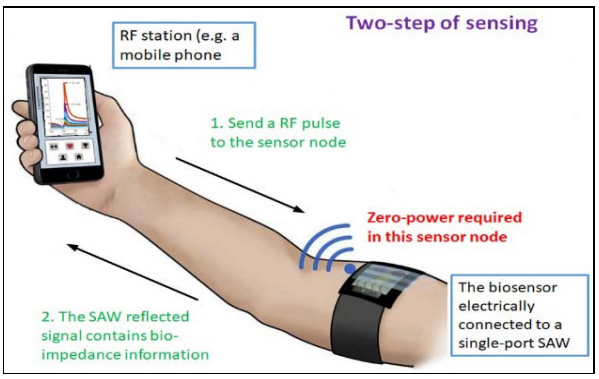

Fig. 1. Proposed remote bioimpedance sensing for zero-power wearable application of biosensors.

This paper investigates the feasibility of a novel surface acoustic wave (SAW) resonator-coupled biosensor for zero-power wearable applications. The transmission methodology is composed of two sensing steps as shown in Fig. 1. In the first step, an industrial science and medical (ISM) band radio frequency (RF) signal is sent to the SAW linked biosensor (zero-power sensor side). In the second step, impedance information of the biosensor coupled to the SAW will then be acquired from the SAW via the reflected RF. The paper is organized as follow: Section II analyses the sensitivity and signal to noise ratio (SNR) of the impedance loaded dual port SAW and the single port SAW resonator coupled impedimetric biosensor to determine the optimum technical approach for remote impedance sensing for zero-power wearable application of biosensors. Section III describes the bioimpedance sensing experiments. The ZnO nanoparticle biosensor preparation and its characterization have been reported. The biosensor was adapted to detect C-reactive protein (CRP) in a concentration range of 0.1 to 2 ng/ml. CRP was selected as a model analyte to illustrate the principle of the remote sensing technique. The rest of the session provides the sensing experiments when the biosensor is connected to a SAW resonator. Measurements of the SAW's resonant frequency shift, to validate remote zero-power SAW impedimetric biosensing method of biosensors, when the concentration of CRP is varied, are described. Section VI concludes the paper.

II. Passively Sensing Bioimpedance of Biosensors

The impedance of a biosensor can be measured in either non-Faradaic or Faradic mode. Using a non-Faradaic biosensor, the impedance measurement is made without the need of a reference electrode and a supporting electrolyte (which are required in the Faradaic mode) and is suited to miniaturization. The addition of a biological sensing layer on or above the electrodes can be used in a non-Faradaic system to measure an impedance spectrum and identify changes in impedance at

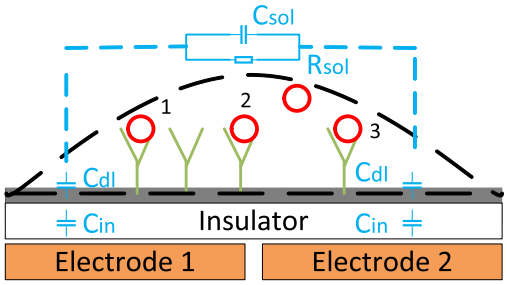

Fig. 2. Schematic of the biosensor. The green symbol represents the bioreceptor and red one represents the target in the sample droplet. The effective bindings of 1, 2 and 3 (red + green) will change the dielectric constant of the solution. At a higher frequency (e.g. hundreds MHz) the dominant impedance component will be the C_{sol}.

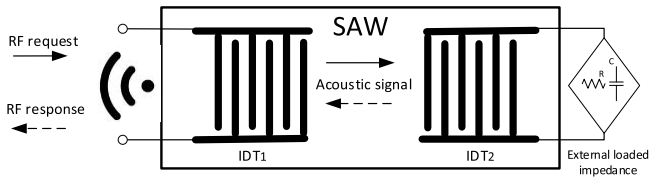

Fig. 3. Schematic layout for passive detection of impedance load.

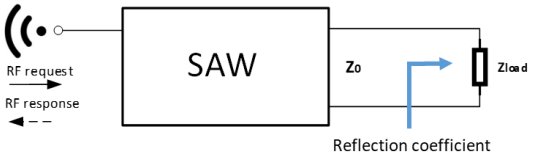

Fig. 4. Equivalent electrical circuit of the impedance loaded SAW sensor.

certain frequencies that are due to interactions on the biosensor surface with target molecules present in the fluid sample. The impedance spectra are presented as a Nyquist chart or as amplitude and phase curves of the impedance [18], [19]. A cluster of curves can be obtained when the concentration of the target molecule in solution is changed. The impedance change of a biosensor is mainly caused by the change in the number of biological interactions, or binding events, where concentration dependent numbers of target molecules or cells are captured on the biosensor surface. In some instances, impedance changes are seen when a single cell, such as a bacterium, is captured on the biosensor surface. Small changes in the number of binding events can result in small changes of both resistance and capacitance (such as fF change in capacitance for a single cell binding [20]) which require more accurate measurements. Fortunately, unlike a resistor which has a constant impedance at different frequencies, the impedance of a capacitor is frequency dependent. So a well-chosen working frequency, specific to the targeted capacitance range, could ensure that the magnitude of impedance is well fitted into the dynamic range of the measurement circuits to achieve a better measurement accuracy. Measurement frequency in biosensing applications have been reported in tens~hundreds MHz for IC based biosensors [7], [20], [21], where two measurement electrodes are placed underneath an insulation layer to measure capacitance of a biosensor, since the dielectric constant of the solution changes with the total numbers of binding events on the sensor [20]. This contactless impedance measurement of a biosensor has also been reported as capacitive biosensors [22], [23].

The schematic of the capacitive biosensor is shown in Fig. 2, where measured capacitance comprises three types of series capacitors including the fixed dielectric constant insulation capacitance C_{in}, the double layer capacitance C_{dl} formed at the contact surface between the sensor surface and solution, and the variable C_{sol} which reflects the variation of the numbers of biological binding events through the change of solution dielectric constant. The reported value of C_{in} and C_{dl} are in μF and C_{sol} is in fF $\sim$ pF and R_{sol} is in MΩ [18], [20]. Therefore at high frequency the impedance of a biosensor is dominated by the tiny capacitor of C_{sol} whose capacitance range of fF $\sim$ pF is feasible to be loaded to a SAW working at hundreds MHz for the purposed of bioimpedance sensing.

A. Sensing Impedance Through a Impedance Loaded SAW

SAW devices use piezoelectric materials (such as quartz, lithium niobate, lithium tantalate, lanthanum gallium silicates) to convert acoustic waves to electrical signals and vice versa through one or more inter-digital-transducers (IDTs) [24]. A schematic of an impedance loaded SAW device [25]–[27] is shown in Fig. 3, where the SAW is configured as a delay-line. In the impedance loaded SAW device's sensing applications, IDT_1 is used to connect to an antenna for communication and while the IDT_2 is used to connect to the impedance load.

When considering the above dual port SAW as a RF black box (e.g. employed as a RF filter or a RF delay line), Fig. 3 can be simplified as Fig. 4, where an impedance load is applied to the output of the SAW which has an electrical output impedance of Z_0. Due to the impedance mismatch, RF reflection happens and the reflection coefficient parameter Γ ($0 < \Gamma \leq 1$) can be expressed as,

$$\Gamma = \left|\frac{Z_{load} - Z_0}{Z_{load} + Z_0}\right| = \left|\frac{\frac{Z_{load}}{Z_0} - 1}{\frac{Z_{load}}{Z_0} + 1}\right| \tag{1}$$

Therefore the RF response signal which is the reflected RF request signal modulated by IDT_2 connected impedance load, conveys information of loaded impedance. The sensitivity of the reflection can be expressed as

$$\frac{d\Gamma}{dZ_{load}} = \frac{2Z_0}{(Z_{load} + Z_0)^2} = \frac{2Z_0}{Z_{load}^2 + Z_0^2 + 2Z_{load}Z_0} \leq \frac{2Z_0}{2Z_{load}Z_0 + 2Z_{load}Z_0} = \frac{1}{2Z_{load}} \tag{2}$$

Therefore the reflection sensitivity is inversely proportional to Z_{load} and the maximum sensitivity occurs when $Z_{load} = Z_0$. However at high sensitive region of $Z_{load} \approx Z_0$, the reflection coefficient Γ is almost zero (refer to (1)) indicating that the reflected signal is very weak at a high sensitivity. This weak signal arises a signal to noise ratio (SNR) issue in the measurement process. To get a measureable reflection signal, Z_{load} value should be not too close to Z_0. Assume $Z_{load} > Z_0$, the sensitivity of $d\Gamma/dZ_{load}$ in (2) becomes

$$\frac{2Z_0}{(Z_{load} + Z_0)^2} < \frac{2Z_0}{(Z_0 + Z_0)^2} = \frac{1}{2Z_0} \tag{3}$$

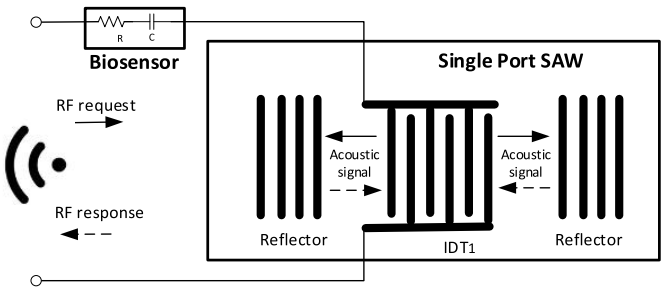

Fig. 5. Proposed biosensor coupled SAW resonator for passive bioimpedance sensing of a biosensor.

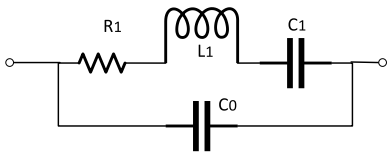

Fig. 6. Electrical equivalent model of a SAW resonator.

In commercially available SAW devices, Z_0 is normally designed as 50 Ω, so the best sensitivity of the impedance loaded SAW device is 1% which happens when $\Gamma \approx 0$. Therefore an impedance loaded SAW device which has been widely used for sensing resistive, capacitive and inductive impedance loads is not suitable for high sensitivity measurements of biosensors (e.g. measuring impedance changes associated with binding of antibodies to specific antigens, ranging from molecules to cells [17], [18]).

B. Bioimpedance Sensing Using a SAW Resonator

Unlike a resistive impedance load, the fF-pF level changes in capacitance of an impedimetric biosensor might be passively measured if a biosensor is connected to a SAW resonator for frequency pulling. When a SAW resonator is connected to the biosensor, as shown in Fig. 5, the resonant frequency of this SAW will be shifted. This shifted resonant frequency can be sensed more accurately than sensing the reflection coefficient in the impedance loaded SAW device.

The typical electrical model of the SAW resonator [28] is shown in Fig. 6, which is composed of motional capacitor C_1 in series with a motional inductor L_1 together in parallel with a static capacitor C_0. The acoustic loss is represented by a series resistor R_1 connected to the other two motional elements (L_1, C_1). The impedance Z and admittance Y of the SAW and the series resonant frequencies (ω_r) and the anti-resonant frequency (parallel resonant frequency ω_a) are expressed as,

$$\begin{aligned} Z &= \frac{1-\omega^2 L_1 C_1 + j\omega R_1 C_1}{-\omega^2 R_1 C_0 C_1 + j\left(\omega C_0 + \omega C_1 - \omega^3 L_1 C_0 C_1\right)} \\ \omega_r &\cong \frac{1}{\sqrt{L_1 C_1}} \\ \omega_a &\cong \frac{1}{\sqrt{L_1\left(\frac{C_0 C_1}{C_0+C_1}\right)}} = \omega_r\sqrt{1+\frac{C_1}{C_0}} \end{aligned} \tag{4}$$

and the admittance Y= $1/Z$.

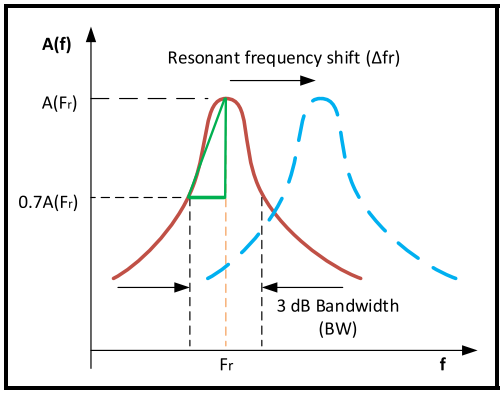

Fig. 7. Resonant property and resonant frequency of the biosensor connected SAW showing resonant frequency shifts with the impedance load change in the biosensor.

According to (4), the parallel loaded connection will not affect the resonant frequency, F_r. The resonant property and resonant frequency shift of the SAW resonator associated with the serially connected biosensor are shown in Fig.7. The increase in resonant frequency can be simply considered as the C_1 and C_{load} in series to give an effective C_1' to determine the new resonant frequency. In this case, the IDT converted signal amplitude is denoted as A(f) and resonant frequency is denoted as F_r. When the peak area of the resonant curve is approximated as a triangle, the simplified conversion function of SAW resonant can be expressed as,

$$\begin{cases} A\left(f_x\right) \approx \dfrac{0.3A\left(F_r\right)}{\frac{BW}{2}}\left[\dfrac{BW}{2} - \left(F_r - f_x\right)\right] \\ Q = \dfrac{F_r}{BW} \end{cases} \tag{5}$$

where BW denotes the 3-dB bandwidth of resonant frequency, Q denotes the quality factor of the curve, f_x denotes the frequency of the RF request signal chosen in resonant bandwidth, and $\max[A(f)] = A(F_r)$. From (5) we have,

$$A\left(f_x\right) \approx 0.3A\left(F_r\right)\left[1 - 2Q\left(1 - \frac{f_x}{F_r}\right)\right] \tag{6}$$

The frequency detection sensitivity is expressed as

$$\frac{d\left[A\left(f_x\right)\right]}{d\left(f_x\right)} = 0.6A\left(F_r\right) \times \frac{Q}{F_r} \tag{7}$$

where $A(F_r) \leq 1$ due to the signal loss. Given that Q of a SAW resonator is around 10^4 and when F_r is at hundreds of MHz, the frequency sensitivity of the SAW coupled biosensor is of the order of 10^{-5}. When a capacitor load can make 1 kHz resonant frequency shift (corresponding to $1/10^5$ change of the resonant frequency of a SAW resonator working at 100 MHz), the measurement sensitivity for the biosensor will achieve 10^{-2} which is the best sensitivity that the impedance loaded SAW device can achieve under a very weak (almost zero) reflected signal. The high sensitivity of the proposed method comes without SNR issues since the measurement signal is within the resonant bandwidth. Additionally, the resonant curve shown in Fig.7 enables the frequency scan to measure multiple points on the curve for detecting the resonant frequency, which is more noise tolerant than the impedance

TABLE I
COMPARISON OF IMPEDANCE LOADED SAW AND BIOSENSOR CONNECTED SAW RESONATOR FOR BIOSENSING

	Impedance loaded SAW	SAW resonator
Numbers of IDTs	2	1
Load connection way	Parallel	Series
Sensitivity	low	high
SNR	low	high

loaded SAW device where only one measurement point is available for a given impedance load. The only drawback is that a frequency scan is necessary for the proposed method since with a fixed frequency RF request signal, there is no guarantee that this frequency drops in the 3 dB bandwidth of the shifted resonant curve when the load capacitance of the biosensor changes.

Based on the high sensitivity and higher SNR which is desired for further signal processing for impedance sensing (either using phase shift or frequency shift detection), the resonant SAW-coupled biosensor is the better choice for sensing impedance changes of a biosensor with varying concentrations of the target analyte. This is due to the fact that the corresponding changes of resistance and capacitance are extremely small and accordingly, a high SNR measurement system is required. The technical summary of the impedance loaded SAW sensor and SAW resonator connected biosensor is listed in Table I.

III. EXPERIMENTS

A. Biosensor Preparation and Validation

The nano-composite impedimetric biosensors were fabricated using 0.15 g ZnO nanoparticles (99.9 + %, 80–200 nm from US Research Nanomaterials Inc., Houston, TX, USA) added to 15 ml double deionized water and 0.1 g CuO nanoparticles (99.5 + %, width 10–30 nm, length: 200–800 nm, long fibrous shape from US Research Nanomaterials Inc.) added to 10 ml double deionized water. The suspensions were stirred at room temperature for 1 hour. From these suspensions a mixture of a volume ratio 2:1 ZnO/CuO was prepare which contained 33% CuO. A 1.5 ml aliquot was ultra-sonicated for 7 periods of 20 s, at 4 min intervals using an exponential microprobe (Soniprep 150) at 30 watts. 200 μl of each suspension was dropped on to clean polyethylene terephthalate (PET) substrates (20 mm x 20 mm) separately to make ZnO/CuO nano-surfaces. These were dried in an oven at 65^{o}C for 80 min and cooled to room temperature, then stored in a dry atmosphere with silica gel for up to 2 days [30]. The sensing area (10 mm x 4 mm) of each ZnO–CuO nano-surface on PET was defined by tape. Subsequently, 40 μl (100 ng or 200 ng) of monoclonal mouse anti-human C-reactive protein (CRP) from HyTest Ltd. (Turku, Finland) was added to the surface. A tapping mode atomic force microscope (AFM) image of the ZnO surface with immobilised antibody shows multiple spikes on the surface is illustrated in Fig. 8. Each spike has an approximate height of 10–15 nm which is consistent with the molecular dimensions of an antibody molecule. The biosensor was then dried in a desiccator with silica gel at 4^{o}C for 18 h. The nano-surface biosensors were then aligned above a pair of D-shape electrodes to perform impedance measurements [31].

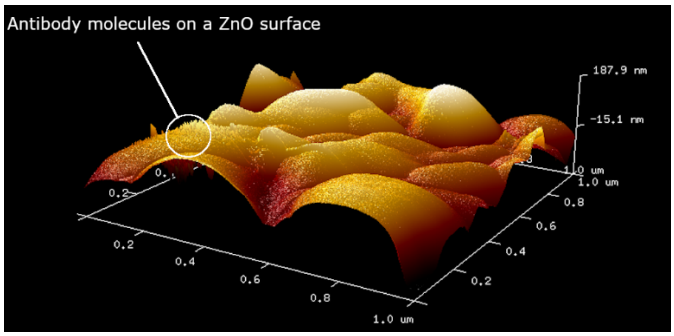

Fig. 8. AFM imaging of the biosensor showed antibody molecules embedded into ZnO surface.

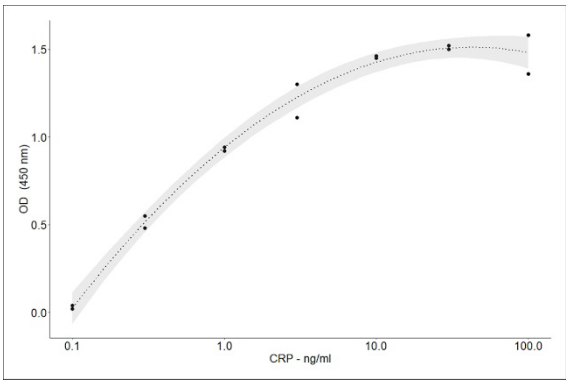

Fig. 9. The dose response of CRP in an ELISA to verify that the anti-CRP antibody captured CRP with the 95% confidence interval for the line of best fit.

The reactivity of the anti-CRP was verified using a sandwich enzyme linked immunosorbent (ELISA) assay. Briefly, the anti-CRP was immobilised on the bottom of a 96-well ELISA plate using 0.1 M carbonate buffer, pH 9.2. Following an overnight incubation, the wells were washed and then blocked with 1% bovine serum albumin in physiological phosphate buffered saline (assay buffer) for 1 hour. The wells were once more washed before samples containing increasing concentrations of CRP were added to wells in the ELISA plate. The plate was incubated for 1 hour at room temperature and the washed 3 times with assay buffer before a second antibody with a covalently coupled enzyme label (horse radish peroxidase) was added for 1 hour. The plates were washed 3 times with assay buffer before an enzyme substrate was added to develop a colour. In this case TMB (3,3′,5,5′-tetramethylbenzidine) was used and after 10 minutes, 0.1 mM sulfuric acid was used to stop the reaction and produce a blue colour, the intensity of which was measured at 450 nm. Fig. 9 shows the optical density at 450 nm of the ELISA plate wells with the different concentrations of CRP added. This clearly shows that as more CRP was added there was an increase in colour produced showing that the CRP was being captured by the antibody immobilised in the ELISA plate wells. The results show that the antibody added to the ELISA plate wells became saturated with the addition of 30 ng/ml CRP to the wells.

A further study was undertaken to demonstrate that antibody could be immobilised on the surface of the

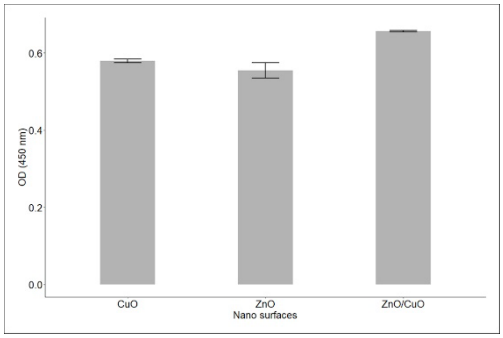

Fig. 10. Bar chart of protein uptake on three nano -surfaces expressed by colour formation at 450 nm from a captured enzyme molecule. n=2.

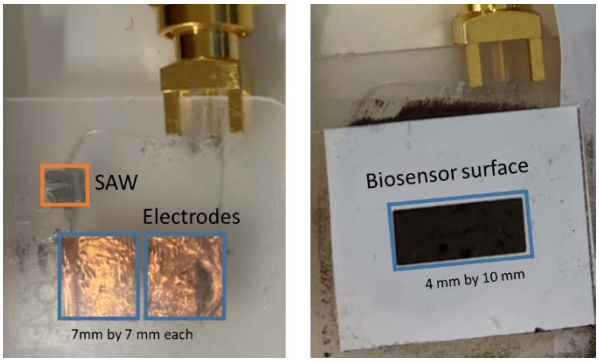

Fig. 11. Experiment set-up for bioimpedance sensing of a biosensor. Left: SAW connected to electrodes. Right: a biosensor is placed on the top of the electrodes to measure frequency shift when the known concentration solution dropped on the surface of the biosensor changes.

ZnO/CuO composite. In this case 75 μl enzyme labelled antibody (2.5 ng/μl) was dropped on to the biosensor surface and allowed to dry in a desiccator overnight. Following a thorough wash to remove any unbound antibody, 3,3′,5,5′-tetramethylbenzidine (TMB) was added as the enzyme substrate to generate a coloured product. After 10 mins 0.1 mM sulfuric acid was added to stop the reaction and produce a blue colour, the intensity of which was read at 450 nm. For comparison the test was also performed on pure ZnO and CuO surfaces.

The results shown in Fig.10 indicate that all the nano-surfaces were capable of capturing antibody on their surface, even using a simple drying technique. The blanks (surface with no antibody) all gave results <0.06 OD units. Although all the surface showed protein uptake, the ZnO/CuO surface used in this paper had a significantly greater protein uptake (18% more than ZnO and 13% more than CuO). The protein absorption on the nano-surfaces could be explained by the fact that ZnO and CuO will have a positive charge on their surface at the pH 7.4, the pH of the assay buffer, while proteins generally have a negative charge at this pH.

B. Measuring Resonant Frequency Shifts Induced by Bioimpedance Change of the Biosensor

To measure the developed biosensor, the electrodes shown in Fig.2 have been assembled as shown in the left of Fig.11, where two 7 by 7 mm metal pads have been placed in close

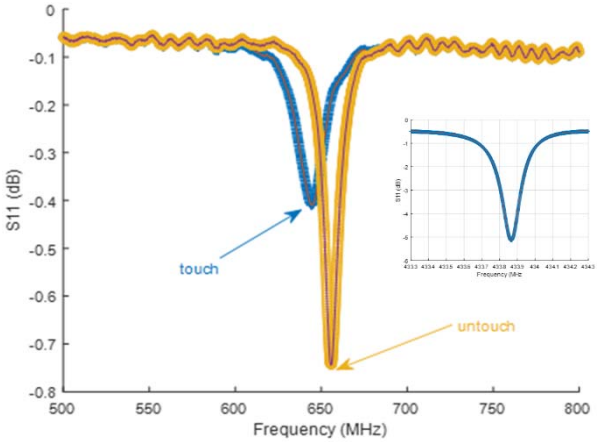

Fig. 12. Parameter S_{11} measured from the network analyzer, demonstrates a 149.8 KHz shift in the resonant frequency for per fF capacitance change by directly fingering touch the electrodes to change the capacitance. The inset showed the measured S_{11} of the original SAW without a capacitive load.

proximity underneath a transparent plastic plate to form the electrodes of the biosensor. The SAW device (EPCOS R900, 433.92 MHz, Q = 12000) has been connected in series to the biosensor. An SMA connector is used to connect the SAW biosensor to the network analyzer of Anritsu MS46121B (1 port USB VNA) to measure the S_{11} parameter, which is the ratio of the reflected signal power to the input power, to determine the resonant frequency of the biosensor-connected-SAW. The wireless transmission has not been included in this paper, since the wireless connection is a well-established technology to replace the cable connections between the SAW-connected biosensor and the network analyzer.

The commercially available smallest capacitor component is in pF level, which is relatively large to validate the SAW biosensor application, where capacitance change is in nF or even fF. Therefore to validate that the load capacitance change can be reflected by the resonant frequency change, the mutual capacitance of a touch sensor used in display [32] has been employed. The electrodes shown in the left of Fig.11 are treated as a capacitive touch sensor, whose capacitance changes when it is touched by a finger. The measured capacitance between two electrodes setting shown in the left of Fig.11 by the LCR meter of E4980A from Keysight is 145.6fF without a finger touching and 69.7 fF when touched. So the resonant frequency shift produced by the fF level capacitance change can be measured. The measured reflection parameter of S_{11} shown in Fig.12 demonstrated an 11.368 MHz resonant frequency shift (from the resonant frequency of 655.737 MHz without touch). From the capacitance change and frequency shift data, the estimated measurement resolution of the SAW biosensor is 149.8 KHz change in the resonant frequency for each fF capacitance change, when simple assumption that the change is linear is applied. This demonstrates that the proposed method is very sensitive to measuring the tiny capacitance change of the biosensor. It is worth noting that the amplitude of the peak of the curve changes as the frequency shifts. Here we are focusing on the detection of the resonant frequency,

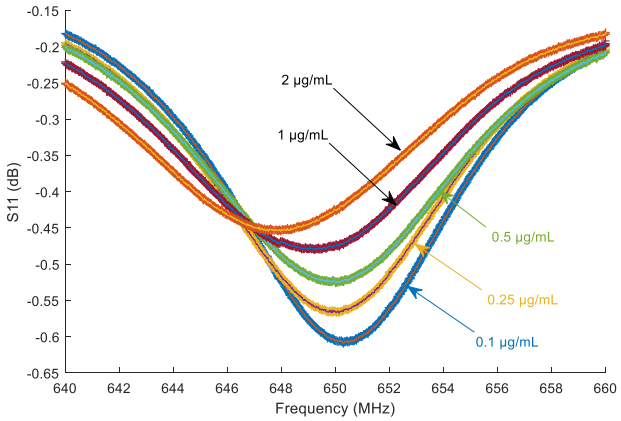

Fig. 13. Resonant frequency changes under different test conditions. It clearly showed that the resonant frequency changes with the concentration: the higher the concentration, the lower the resonant frequency.

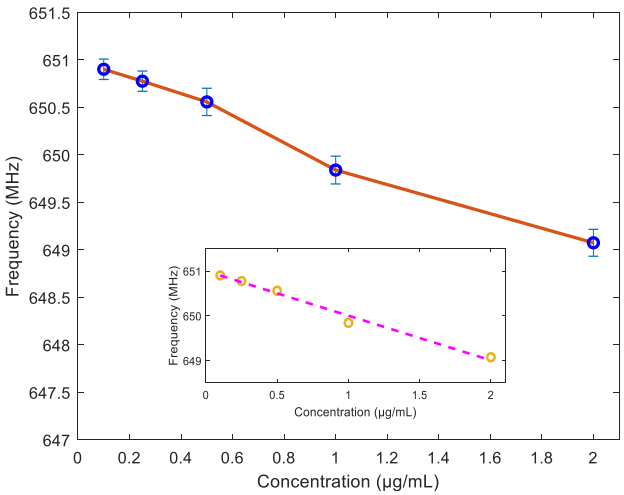

Fig. 14. Resonant frequency changes for different CRP concentrations, 0.1. 0.25, 0.5. 1, and 2 μg/ml, and (inset) linear fit to the data.

TABLE II
RESONANT FREQUENCY (f0: MHz) OF A BISOSENSOR WHEN DIFFERENT CONCENTRATION OF CRP PROTEIN (μg/ml) IS APPLIED

Concentration	0.1	0.25	0.5	1	2
f0 for test1	650.934	650.469	650.293	649.661	648.918
f0 for test 2	650.594	650.481	650.109	649.325	649.046
f0 for test3	651.026	650.837	650.625	649.225	647.918

so the amplitude change is not critical as long as the peak of the curve can be detected.

Bio-impedance sensing experiments have been performed in which a set of concentrations (0.1, 0.25, 0.5, 1, 2 μg/ml) of the target protein, CRP, in solution are applied to the surface of the biosensor. Fig. 13 demonstrated a typical S_{11} parameter recorded from a biosensor, which clearly shows the resonant frequency change with concentration change of the solution. The frequency range shown in the figure has a 20 MHz span, so when the frequency range is selected as 640-660 MHz and the number of data points of the network analyzer is selected as 20,000, the measured data has a 1 KHz frequency resolution. The resonant frequency (in MHz) detected from the curves are: 650.293, 650.117, 650.009, 649.225, and 647.092 corresponding to the concentration of 0.1, 0.25, 0.5, 1, 2 μg/ml, respectively. This demonstrated that even when concertation changes from 0.1 to 0.25 μg/ml, there is a frequency change of 176 KHz, which can be easily detected by RF receiver circuits in the RF station [13].

The test results of the resonant frequencies of three replicate measurements from a biosensor are listed in Table II. It can be seen that the resonant frequency decreases with concentration in all cases, indicating after two times reuse, the biosensor is still functional. However, the frequency shifts are not proportional for all cases, hence it is recommended not to re-use a biosensor for precise measurements. The data shown in the table also suggests that to have reliable measurement results, multiple readings for every test point are required, so an average value can be obtained to reduce the standard deviation of the observed value [33].

The test results from 10 biosensors are shown in Fig. 14. It demonstrated the resonant frequency shifts with the applied analyte concentration. The averaged resonant frequencies of 10 sensors are 650.9019, 650.7766, 650.5584, 649.8406, and 649.0744 MHz corresponding to the concentration of 0.1, 0.25, 0.5, 1, 2 μg/ml CRP, resulting in the resonant frequency shifts of -125.3 KHz for the concentration change from 0.1 to 0.25 μg/ml, -218.3 KHz for the concentration change from 0.25 to 0.5 μg/ml, -717.7 KHz for the concentration change from 0.5 to 1 μg/ml, and -766.3 KHz for the concentration change from 1 to 2 μg/ml. Although the relationship between the CRP concentration and resonant frequency is not exactly linear, the resolution showed in the curve (e.g. the minimum 76 KHz resonant frequency change for per 0.1 μg/ml concentration change) clearly demonstrated that the proposed method is sensitive enough for sensing the impedance change of the biosensor in the relevant clinical range, in a zero-power way, where a passive SAW device is used as the RF reflector which carries the impedance information in the reflected RF signal.

The fitted line of $y = 651 - 0.9898 \times x$ where y denotes the resonate frequency in MHz and x denotes the CRP concentration in μg/ml, shown in the inset figure, demonstrates a statistical result of about 99 KHz frequency shift for 0.1 μg/ml concentration change. Based on the 146.5 KHz maximum standard deviation (σ) shown in Fig.14, the limit of detection of the experiment is 0.6 μg/ml with a confident level higher than 95% when $\pm 2\sigma_{\max}$ (586 KHz, corresponding to 0.59 μg/ml when using the slop of 0.9898 MHz/(μg/ml)) is considered, while the resonant frequency at each test point in Fig.14 showed that a measurement resolution of 0.1 μg/ml has been achieved.

The 0.59 μg/ml measurement accuracy achieved in this method, when compared to the 149.8 KHz/fF frequency shift shown in Fig.12, results in a capacitance measurement accuracy of 586/149.8 = 3.9 fF with a resolution of 1000 aF/149.8 = 6.7 aF since every 1KHz frequency change can be detected. Given that for most of the biosensing applications, the required capacitance resolution is in hundred nF [34], the

TABLE III
PERFORMANCE COMPARISON

	Measurement resolution	Implementation
Ref [34]	nF (10^{-9})	Components
Ref [23]	pF (10^{-12})	Microfluidic chip
Ref [20]	450 aF (10^{-18})	Transistors (CMOS)
Ref [37]	1 aF (10^{-18})	Transistors (CMOS)
This work	6.7 aF (10^{-18})	Components

aF level capacitance measurement resolution achieved by this method even matches the level of the CMOS based capacitive sensors [35], [36], demonstrating a very sensitive measurement method for capacitive biosensors. The performance comparison of this method to other reported ones are listed in Table III.

The proposed measurement also makes it possible to miniaturize biosensors for area-restricted applications or to reduce the fabrication cost since a small surface area with a smaller capacitance change can be detected by this new method. Similarly, it also implies that the system will be appropriate for detection of other analytes where the required lower limit of the measurement range is <1 ng/ml.

C. Discussion

Introducing a RF link to replace the communication cable between the SAW connected biosensor and the other test circuits to achieve the proposed full passive bioimpedance sensing should be straightforward, since remotely passive SAW applications has been widely reported [13], [16], [26], [38]–[41]. However, when considering that there is about 4.75 dB peak attenuation introduced by the biosensor (−5.15 dB shown in the inset of Fig.12 when no-load is attached to the SAW and the minimum −0.4 dB shown in the Fig.13), the read distance which is composed of the communication from the reader to the SAW and then from the SAW to the reader can be a concern. The read distance R of a SAW has been expressed in [42], which showed that

$$P_R = G\frac{P_T\lambda^2}{R^4} \tag{8}$$

where P_T denotes the transmission power and P_R denotes the received power at the read point, λ denotes the wavelength of the RF signal (calculated by the RF frequency f using $C = f\lambda$, $C = 3 \times 10^8$ m/s), and G is a constant related to the RF system set-up including the antenna gain and other parameters. Formula (8) means that to keep the same SNR in the instrumentation side, the relationship between the new read distance R_1 for SAW connected biosensor and the R_0 for the SAW without a load in this application will become, $R_1 = (P_{R0}/P_{R1})^{-1/4} R_0 = (10^{4.75/10})^{-1/4} R_0 = 76\% R_0$. Given that the achieved read distance of 2.5 m in the 433 MHz band [43], the read distance of the SAW connected biosensor will be 2.5 m × 76% = 1.9 m. Even considering an extra insertion loss of 20 dB, the read distance will be reduced to 60 cm which is still better than other RFID solutions. In addition, using 868 (865-868) MHz ISM band where transmission power limitation has been increased from 25 mW to 2000 mW [44], will be a choice to increase the read distance (according to formula (8)) when communication distance becomes a concern.

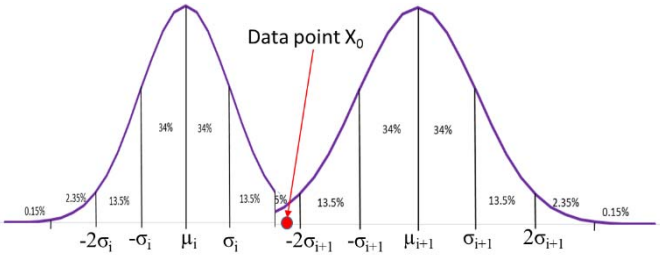

Fig. 15. Determining the measurement accuracy by considering the probability distribution of two adjacent measurement points.

Although the reported experiment have not included concentration steps of 0.59 μg/ml, the claimed accuracy of 0.59 μg/ml which is concluded from the statistics of the measurements, is reliable. Considering that when the distance of $4\sigma_{max}$ (σ_{max} is the maximum standard deviation of the 5 test points: $\sigma_{max} = \max(\sigma_1, \sigma_2, \ldots\sigma_5)$) is applied to the two adjacent test points (both measurement data sets obey the normal distribution) of i (μ_i, σ_i) and i+1 (μ_{i+1}, σ_{i+1}) as shown in Fig.15, the error of counting one measurement data x_0 ($\mu_i \le x_0 \le \mu_{i+1}$) into the incorrect data point which most probably happens in the intersection area of the Fig. 15 can be calculated as,

$$P_{err} = \begin{cases} \displaystyle\int_{-\infty}^{x_0} \frac{1}{\sqrt{2\pi}\sigma_{i+1}} \exp\left[\frac{(x-\mu_{i+1})^2}{2\sigma_{i+1}^2}\right] dx \\ \quad \mu_i \le x_0 < \mu_i + 2\sigma_{max} \\ \displaystyle\int_{x_0}^{\infty} \frac{1}{\sqrt{2\pi}\sigma_i} \exp\left[-\frac{(x-\mu_i)^2}{2\sigma_i^2}\right] dx \\ \quad \mu_i + 2\sigma_{max} \le x_0 \le \mu_{i+1} \end{cases} \tag{9}$$

Given that [45]

$$\int_{\mu_i-2\sigma_i}^{\mu_i+2\sigma_l} \frac{1}{\sqrt{2\pi}\sigma_i} \exp\left[-\frac{(x-\mu_i)^2}{2\sigma_i^2}\right] dx > 95\% \quad (i = 1, 2 \ldots 5) \tag{10}$$

and $\mu_{i+1} - \mu_{i} \ge 4\sigma_{max}$, it can be concluded that P_{err} in formula (9) is less than 5% and therefore the measurement data will be reliable to free the measurement uncertainty concern.

The sensitivity calculated by formula (7) for this experiment where almost a hundred KHz frequency shift for 0.1 μg/ml CRP, demonstrated that the proposed method has a much higher sensitivity than the best sensitivity of the impedance loaded SAW. However, in a series resonant circuit, the voltage applied to a single component may be much higher than the voltage applied to the circuit. Hence, in this system a safety concern is raised, since biosensor is in series with the SAW. Given that the RF excitation is limited to 25 mW for the 433MHz ISM band wireless communication, the allowed maximum amplitude of the RF excitation can be 1.12V at 50Ω impedance. Even with twice the total voltage applied to the biosensor, it is still a safe voltage to keep the leakage current

to human body below 10 mA specified by IEC60601 for MHz RF signals [5]. Therefore it is safe to series connect a biosensor working at hundreds of MHz and a high frequency SAW for passive bioimpedance sensing.

The reflection strips of the reflector shown in Fig. 5, have a fixed gap designed for the resonant frequency. In our applications the resonant frequency has been largely shifted from the original value due to the connected biosensor. This shifted frequency will produce a phase shift from each reflecting strip, making the reflected RF signal waveform slightly distorted. However, when considering that frequency shift detection is implemented in the frequency domain, the phase shift should not affect the power spectrum of the reflected RF signal. The spectrum $F(\omega)$ of the reflected RF signal with a phase shift φ_0 at the second reflect strip of N strips is calculated as,

$$\begin{aligned} F(\omega) &= \int_{-\infty}^{+\infty} \sum_{n=1}^{N} \frac{1}{N} \cos\left(\omega_0 t + (n-1)\varphi_0\right) e^{-j\omega t} dt \\ &= \frac{1}{N}\left(\int_{-\infty}^{+\infty} \cos\left(\omega_0 t + \varphi_0\right) e^{-j\omega t} dt + \cdots \right. \\ &\quad \left. + \int_{-\infty}^{+\infty} \cos\left(\omega_0 t + N\varphi_0\right) e^{-j\omega t} dt\right) \\ &= \frac{e^{j\varphi_0} + e^{j2\varphi_0} + \cdots + e^{j(N-1)\varphi_0}}{2N} \delta(\omega - \omega_0) \\ &\quad + \frac{e^{-j\varphi_0} + e^{-j2\varphi_0} + \cdots + e^{-j(N-1)\varphi_0}}{2N} \delta(\omega + \omega_0) \end{aligned}$$

where

$$\delta(\omega) = \int_{-\infty}^{+\infty} e^{-j\omega t} dt \tag{11}$$

and the reflection coefficient of N reflection strips are assigned as identical.

For power spectrum of $|F(\omega)|$, since $|e^{j\varphi|} = 1$ for arbitrary φ, when $(N-1)|\varphi_0| < \pi/2$ the spectrum of the reflected RF signal will not be affected, since in this case

$$\left| \frac{e^{j\varphi_0} + e^{j2\varphi_0} + \cdots + e^{j(N-1)\varphi_0}}{2N} \right| = \frac{1}{2} \tag{12}$$

where φ_0 denotes the resonant frequency shift from the first reflector as

$$\varphi_0 = \frac{\Delta F_r}{F_r} \times 2\pi \times \frac{\lambda/2}{\lambda} = \frac{\Delta F_r}{F_r} \times \pi \tag{13}$$

Apparently the phase shiftφ_0 is almost $\pi/2$ in our experiments so formula (12) is not working. The frequency component of the reflected signal can still be detected without a network analyzer in practical application (refer to Fig. 1) according to formula (11), but the amplitude of the spectrum will be decreased, resulting in a reduced communication distance.

Although in previously reported works, the power consumption of impedance measurement for biosensors has been reduced from mW [6] to μW [7], [18], [20], these systems still require powering of sensor side. For the SAW resonator-coupled biosensor described here, no power source is required at the biosensor node. This is especially important when considering wearable applications where a wireless communication link is required. However, more technical aspects such as introducing a reference measurement channel for calibration of the SAW component parameters change (e.g. variation in initial resonant frequency such as 433.92 MHz ± 75 KHz specified by the EPCOS R900 resonator, temperature related parameters such as −19 ppm/°C resonant frequency change [46]) should be considered for practical use of SAW connected biosensor since SAW device is very sensitive.

IV. Conclusion

SAW resonators have the potential to create biosensing nodes that combine passive impedance sensing and zero power communication when coupled with the capacitive biosensor. This is possible as the process of reflecting the excitation RF signal in the SAW is passive. The SAW reflected RF signal contains impedance information of the biosensor, where changes in the impedance values relate to the variation in the number of binding events on the biosensor surface and thus the concentration of the target analyte. This impedance change can be indirectly acquired by detecting the resonant frequency change of the reflected RF signal at the RF station, e.g. a mobile phone, where power supply is not typically an issue. Therefore, this system is highly suited to wearable biosensor applications which transmit readings of analyte concentrations, for example cortisol levels in sweat on or under the skin, to a mobile device. Biosensing experiments have demonstrated that a single IDT SAW resonator working in hundreds MHz can detect fF level capacitance changes which has only been previously achieved in transistor level circuits. This has allowed changes in CRP concentrations down to 0.6 μg/ml (well below the normal clinical cut-off level) to be detected by the SAW resonator-coupled biosensor, with a zero-power requirement at the biosensor node. In addition, due to the capability of measurement of very small capacitance changes, it is predicted that the system will be appropriate for measurement of other analytes where the clinical range extends down to ng/ml levels.

References

[1] A. J. Bandodkar and J. Wang, "Non-invasive wearable electrochemical sensors: A review," *Trends Biotechnol.*, vol. 32, no. 7, pp. 363–371, Jul. 2014.

[2] J. Kim, R. Kumar, A. J. Bandodkar, and J. Wang, "Advanced materials for printed wearable electrochemical devices: A review," *Adv. Electron. Mater.*, vol. 3, no. 1, Jan. 2017, Art. no. 1600260.

[3] A. J. Bandodkar, W. Jia, and J. Wang, "Tattoo-based wearable electrochemical devices: A review," *Electroanalysis*, vol. 27, no. 3, pp. 562–572, Mar. 2015.

[4] H. Lee *et al.*, "Wearable/disposable sweat-based glucose monitoring device with multistage transdermal drug delivery module," *Sci. Adv.*, vol. 3, no. 3, Mar. 2017, Art. no. e1601314.

[5] X. Yue and C. McLeod, "FPGA design and implementation for EIT data acquisition," *Physiol. Meas.*, vol. 29, pp. 1233–1246, Oct. 2008.

[6] L. J. Koerner and T. W. Secord, "An embedded electrical impedance analyzer based on the AD5933 for the determination of voice coil motor mechanical properties," *Sens. Actuators A, Phys.*, vol. 295, pp. 99–112, Aug. 2019.

[7] A. Manickam, A. Chevalier, M. McDermott, A. D. Ellington, and A. Hassibi, "A CMOS electrochemical impedance spectroscopy (EIS) biosensor array," *IEEE Trans. Biomed. Circuits Syst.*, vol. 4, no. 6, pp. 379–390, Dec. 2010.

[8] X. Yue, J. Kiely, D. Gibson, and E. M. Drakakis, "Charge-based supercapacitor storage estimation for indoor sub-mW photovoltaic energy harvesting powered wireless sensor nodes," *IEEE Trans. Ind. Electron.*, vol. 67, no. 3, pp. 2411–2421, Mar. 2020.

[9] L. Xie, Y. Shi, Y. T. Hou, and A. Lou, "Wireless power transfer and applications in sensor netowrks," *IEEE Wireless Commun.*, vol. 20, no. 4, pp. 140–145, Sep. 2013.

[10] D. P. Rose *et al.*, "Adhesive RFID sensor patch for monitoring of sweat electrolytes," *IEEE Trans. Biomed. Eng.*, vol. 62, no. 6, pp. 1457–1465, Jun. 2015.

[11] M. C. M. Oliveros *et al.*, "Photosensitive chipless radio-frequency tag for low-cost monitoring of light-sensitive goods," *Sens. Actuators B, Chem.*, vol. 223, pp. 839–845, Feb. 2016.

[12] D. B. Go, M. Z. Atashbar, Z. Ramshani, and H.-C. Chang, "Surface acoustic wave devices for chemical sensing and microfluidics: A review and perspective," *Anal. Methods*, vol. 9, no. 28, pp. 4112–4134, 2017.

[13] L. Zou, C. McLeod, and M. R. Bahmanyar, "Wireless interrogation of implantable SAW sensors," *IEEE Trans. Biomed. Eng.*, vol. 67, no. 5, pp. 1409–1417, May 2020, doi: 10.1109/TBME.2019.2937224.

[14] E. R. Gray *et al.*, "Ultra-rapid, sensitive and specific digital diagnosis of HIV with a dual-channel SAW biosensor in a pilot clinical study," *NPJ Digit. Med.*, vol. 1, no. 1, p. 35, Dec. 2018.

[15] R. Steindl, A. Pohl, and F. Seifert, "Impedance loaded SAW sensors offer a wide range of measurement opportunities," *IEEE Trans. Microw. Theory Techn.*, vol. 47, no. 12, pp. 2625–2629, Dec. 1999.

[16] W. Luo, Q. Fu, J. Wang, Y. Wang, and D. Zhou, "Theoretical analysis of wireless passive impedance-loaded SAW sensors," *IEEE Sensors J.*, vol. 9, no. 12, pp. 1778–1783, Dec. 2009.

[17] O. H. Murphy, C. N. McLeod, M. Navaratnarajah, M. Yacoub, and C. Toumazou, "A pseudo-normal-mode helical antenna for use with deeply implanted wireless sensors," *IEEE Trans. Antennas Propag.*, vol. 60, no. 2, pp. 1135–1139, Feb. 2012.

[18] M. Grossi and B. Riccò, "Electrical impedance spectroscopy (EIS) for biological analysis and food characterization: A review," *J. Sensors Sensor Syst.*, vol. 6, no. 2, pp. 303–325, Aug. 2017.

[19] A. Valero, T. Braschler, and P. Renaud, "A unified approach to dielectric single cell analysis: Impedance and dielectrophoretic force spectroscopy," *Lab Chip*, vol. 10, no. 17, pp. 2216–2225, 2010.

[20] N. Couniot, L. A. Francis, and D. Flandre, "A 16 × 16 CMOS capacitive biosensor array towards detection of single bacterial cell," *IEEE Trans. Biomed. Circuits Syst.*, vol. 10, no. 2, pp. 364–374, Apr. 2016.

[21] N. Couniot, D. Bol, O. Poncelet, L. A. Francis, and D. Flandre, "A capacitance-to-frequency converter with on-chip passivated microelectrodes for bacteria detection in saline buffers up to 575 MHz," *IEEE Trans. Circuits Syst. II, Exp. Briefs*, vol. 62, no. 2, pp. 159–163, Feb. 2015.

[22] A. Santos, "Fundamentals and applications of impedimetric and redox capacitive biosensors," *J. Anal. Bioanal. Techn.*, vol. S7, no. 12, p. 16, 2014.

[23] T. V. Quoc, V. N. Ngoc, T. T. Bui, C.-P. Jen, and T. C. Duc, "High-frequency interdigitated array electrode-based capacitive biosensor for protein detection," *BioChip J.*, vol. 13, no. 4, pp. 403–415, Dec. 2019.

[24] A. Pohl, "A review of wireless SAW sensors," *IEEE Trans. Ultrason., Ferroelectr., Freq. Control*, vol. 47, no. 2, pp. 317–330, Mar. 2000.

[25] V. P. Plessky, "SAW impedance elements," *IEEE Trans. Ultrason., Ferroelectr., Freq. Control*, vol. 42, no. 5, pp. 870–875, Sep. 1995.

[26] X. Zhu, J. Xing, L. Xie, and T. Wang, "Analysis and test of a wireless impedance-loaded SAW sensor," *Micro Nano Lett.*, vol. 14, no. 5, pp. 534–537, May 2019.

[27] X. Yue, J. Kiely, C. McLeod, and P. Wraith, "SAW based passively bioimpedance sensing for zero-power wearable applications of biosensors," in *Proc. IEEE Biomed. Circuits Syst. Conf. (BioCAS)*, Oct. 2019, pp. 1–4, doi: 10.1109/BIOCAS.2019.8919051.

[28] K. M. Lakin, "Modeling of thin film resonators and filters," in *IEEE MTT-S Int. Microw. Symp. Dig.*, vol. 1, Jun. 1992, pp. 149–152.

[29] M. O. Sonnaillon and F. J. Bonetto, "A low-cost, high-performance, digital signal processor-based lock-in amplifier capable of measuring multiple frequency sweeps simultaneously," *Rev. Sci. Instrum.*, vol. 76, no. 2, Feb. 2005, Art. no. 024703.

[30] L. Cao, J. Kiely, M. Piano, and R. Luxton, "A copper oxide/zinc oxide composite nano-surface for use in a biosensor," *Materials*, vol. 12, no. 7, p. 1126, 2019.

[31] L. Cao, J. Kiely, M. Piano, and R. Luxton, "Facile and inexpensive fabrication of zinc oxide based bio-surfaces for C-reactive protein detection," *Sci. Rep.*, vol. 8, no. 1, pp. 1–9, 2018.

[32] G. Walker, "A review of technologies for sensing contact location on the surface of a display," *J. Soc. Inf. Display*, vol. 20, no. 8, pp. 413–440, Aug. 2012.

[33] X. Yue *et al.*, "A real-time multi-channel monitoring system for stem cell culture process," *IEEE Trans. Biomed. Circuits Syst.*, vol. 2, no. 2, pp. 66–77, Jun. 2008.

[34] H. Le, J. Park, and S. Cho, "A probeless cpacitive biosensor for direct detection of amyloid bata 1–42 in human serum based on an interdigitated chin-shaped electrode," *Micromachines*, vol. 11, no. 9, pp. 791, Sep. 2020.

[35] S. Forouhi, R. Dehghani, and E. Ghafar-Zadeh, "CMOS based capacitive biosensors for life science applications: A review," *Sens. Actuators A, Phys.*, vol. 297, 2019, Art. no. 111531.

[36] A. Alhosshany, S. Silvashankar, Y. Mashreal, H. Omran, and K. N. Salama, "A biosensor-CMOS platform and integrated readoutcircuit in 0.18-μm CMOS technology for cancer biomarker detection," *Sensors*, vol. 17, p. 1942, Sep. 2017.

[37] F. Widdershoven *et al.*, "A CMOS pixelated nanocapacitor biosensor platform for high-frequency impedance spectroscopy and imaging," *IEEE Trans. Biomed. Circuits Syst.*, vol. 12, no. 6, pp. 1369–1382, Dec. 2018.

[38] J. R. Humphries and D. C. Malocha, "Wireless SAW strain sensor using orthogonal frequency coding," *IEEE Sensors J.*, vol. 15, no. 10, pp. 5527–5534, Oct. 2015.

[39] J. R. Humphries *et al.*, "Noise radar approach for interrogating SAW sensors using software defined radio," *IEEE Sensors J.*, vol. 17, no. 20, pp. 6760–6769, Oct. 2017.

[40] W. Feng, J.-M. Friedt, G. Goavec-Merou, and M. Sato, "Passive radar delay and angle of arrival measurements of multiple acoustic delay lines used as passive sensors," *IEEE Sensors J.*, vol. 19, no. 2, pp. 594–602, Jan. 2018.

[41] S. Kim, H. Wang, I. Park, and K. Lee, "Toward real time monitoring of wafer temperature in plasma chamber through surface acoustic wave resonator and mu-negative metamaterial antenna," *IEEE Sensors J.*, vol. 21, no. 18, pp. 19863–19871, Sep. 2021.

[42] J. D. Griffin and G. D. Durgin, "Complete link budgets for backscatter-radio and RFID systems," *IEEE Antennas Propag. Mag.*, vol. 51, no. 2, pp. 11–25, Apr. 2009.

[43] F. Nawaz and V. Jeoti, "SAW sensor read range limitations and perspectives," *Wireless Netw.*, vol. 20, no. 8, pp. 2581–2587, Nov. 2014.

[44] M. Lauridsen, B. Vejlgaard, I. Z. Kovacs, H. Nguyen, and P. Mogensen, "Interference measurements in the European 868 MHz ISM band with focus on Lora and SigFox," in *Proc. IEEE Wireless Commun. Netw. Conf. (WCNC)*, Mar. 2017, pp. 1–6, doi: 10.1109/WCNC.2017.7925650.

[45] M. DeGroot and M. Schervish, *Probability and Statistics*, 4th ed. Reading, MA, USA: Addison-Wesley, 2019.

[46] G. Ciplys *et al.*, "Temperature coefficent of SAW frequency in single crystal bulk AlN," *Electron. Lett.*, vol. 39, no. 9, pp. 755–757, 2003.

Xicai (Alex) Yue (Senior Member, IEEE) received the B.Eng. degree in telecommunication engineering and the M.Eng. and Ph.D. degrees in biomedical engineering from Xi'an Jiaotong University, Xi'an, China, in 1985, 1995, and 1999, respectively.

He was a University Teaching Assistant and then a Lecturer of Digital Switching in China after graduation. From 1999 to 2016, he was with Tsinghua University, Beijing, China, the Imperial College London, London, U.K., and the Sharp Laboratories of Europe, Oxford, U.K. He is currently a Senior Lecturer and the Head of Instrumentation with the Institute of Bio-Sensing Technology, University of the West of England, Bristol, U.K. He has published more than 20 lead-author peer-reviewed journal articles and an international patent. His current research interests include contactless electrodes for long-term physiological measurements (e.g., ECG, EOG, and EEG), passive communication for human–computer interface, power management for energy harvesting, flexible electronics and mixed-signal CMOS IC design for power/area restricted implantable, and wearable biomedical applications. Dr. Yue is an Associate Editor of the *Measurement* (Elsevier) journal. He was a recipient of the Live Demo Special Session Award of the IEEE International Symposium on Circuits and Systems.

Janice Kiely received the B.Eng. (Hons.) degree in electronic engineering from the University of Sheffield, Sheffield, U.K., in 1987, and the Ph.D. degree from the University of Cardiff, Cardiff, U.K., in 1992.

Her Ph.D. degree involved the development of novel, miniature thermoelectric devices for passive IR detection. She was appointed as a Lecturer in Sensors and Instrumentation in 1993 and subsequently has held the roles of the Head of the Department of Electronic and Computer Systems Engineering and the Head of Research and Knowledge Exchange of the Faculty of Engineering. Since 2008, she has been the Co-Director of the Institute of Bio-Sensing Technology, Bristol, U.K., and since 2016, she has been the Health Technology Hub, University of the West of England. In 2014, she was the Founder of an University spin out, Miatech Biosolutions, Ltd. Dr. Kiely is a Fellow of the Institute of Engineering and Technology, U.K., and in 2015 she was awarded a Royal Academy of Engineering Enterprise Fellowship.

Richard Luxton is the Director of the Institute of Bio-Sensing Technology studied Clinical Chemistry in the National Health Service for 13 years at Bristol Royal Infirmary before moving to the Institute of Neurology, London, to study for a Ph.D. degree in neuro-immunology, investigating antibody affinity in the CSF of patients with multiple sclerosis. At the University of the West of England, he focused his research in the area of developing new rapid detection technologies for point of care diagnostics, environmental analysis, food safety, and homeland defense applications. One area of research that has been particularly successful is the development of magnetic detection technology for use in immunoassays. Other areas of research include the rapid detection of change in cell systems using impedance spectroscopy and novel data interpretation algorithms.

He has led many large multi-partner projects to develop new technology for the rapid detection of analytes and is the Conference Chair the successful International Conference of Bio-sensing Technology and the Editor-in-Chief of the *Journal Sensor and Biosensor Research*.

Boyang Chen received the B.Sc. degree in biomedical sciences from Newcastle University, Newcastle upon Tyne, U.K., in 2016, and the M.Sc. degree in biotechnology from the University of Leeds, Leeds, U.K., in 2017. He is currently pursuing the Ph.D. degree in biotechnology and biosensing with the University of the West of England, Bristol, U.K.

His project title is 'Impedimetric biosensors for the monitoring of cell stress in mammalian cell cultures.' His research interests include electrical impedance spectroscopy, cell death, apoptosis, antibody-based sensors, and development of rapid-detection techniques.

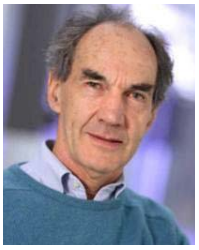

Chris N. McLeod (Member, IEEE) received the M.A. degree in engineering from Cambridge University, Cambridge, U.K., the M.Sc. degree in bioengineering from Strathclyde University, Glasgow, U.K., and the D.Phil. degree in the measurement of the nutritional intake of breast-fed babies. He worked with medical research groups with Oxford University, Oxford, U.K., from 1975 to 1984. He moved to Oxford Brookes University as a Lecturer in Engineering and maintained research collaborations with clinicians in anaesthetics and paediatrics developing minimally invasive devices for intensive care monitoring of adults and neonates, including EIT and EIS systems. Prof. McLeod served as an Associate Editor for IEEE TRANSACTIONS ON MEDICAL IMAGING. He moved to the Imperial College London to develop implantable passive SAW sensors to measure cardiovascular pressures continuously to provide critical clinical information for the management of pharmaceutical therapies. He is one of the founders of Precision Cardiovascular Ltd.

Emanuel Manos Drakakis (Member, IEEE) received the B.S. degree in physics and the M.Phil. degree in electronic physics and radioelectrology from the Aristotle University of Thessaloniki, Macedonia, Greece, and the Ph.D. degree in analog IC design from the Imperial College London, London, U.K. He is currently a Professor in Bio-Circuits and Systems with the Department of Bioengineering, Imperial College London, where he also works as the Deputy Head. In this Department, he has founded the Bioinspired VLSI Circuits and Systems Group, whose research focuses on "Circuits for and from Biology and Medicine." He has authored or coauthored a large number of peer-reviewed papers and several book chapters. He was a recipient of many prizes for research excellence and is involved in several cross-disciplinary, multi-million research projects. He is currently an Associate Editor of Frontiers in *Neuromorphic Engineering*. He is also an Editor of *Measurement* (Elsevier) and an Editorial Advisor of *BMC Biomedical Engineering* and *Nature* (Springer). In the past, he has served as an Associate Editor for IEEE TRANSACTIONS (IEEE TRANSACTIONS ON BIOMEDICAL CIRCUITS AND SYSTEMS (IEEE TBIOCAS), IEEE TRANSACTIONS ON CIRCUITS AND SYSTEMS—I: REGULAR PAPERS (IEEE TCASI), and IEEE TRANSACTIONS ON CIRCUITS AND SYSTEMS—II: EXPRESS BRIEFS (IEEE TCAS-II) for a total of 19 years, a Subject Editor with *International Journal of Electronics* and a Guest Editor with IEEE COMMUNICATIONS LETTERS. He has a Cumulative Editorial Service to the research community of more than 33 years.